Proposal for simultaneous all-optical AND, NOR, and XNOR logic gates using QPM cascading nonlinear effects in two PPLNs

Yubin Tang (唐喻斌), Yuping Chen (陈玉萍)*, Haowei Jiang (蒋浩苇), Weifeng Ji (吉唯峰), Yijing Wu (吴依菁), and Xianfeng Chen (陈险峰)**

State Key Laboratory on Fiber Optic Local Area Communication Networks and Advanced Optical Communication Systems, Department of Physics, Shanghai Jiao Tong University, Shanghai 200240, China

**Corresponding author: ypchen@sjtu.edu.cn; **corresponding author: xfchen@sjtu.edu.cn*

Received December 8, 2012; accepted February 25, 2013; posted online May 30, 2013

We propose AND, NOR, and XNOR logic gates realized simultaneously for 40-Gb/s networks, in which the realization of NOR and XNOR logic gates using only MgO-doped periodically poled lithium niobate (MgO:PPLN) is reported. In our configuration, we exploit broadband quasi-phase matching (QPM) cascaded second harmonic and difference-frequency generation (cSHG/DFG), cascaded sum-frequency and difference-frequency generation (cSFG/DFG) in one MgO:PPLN, and the narrow band QPM sum-frequency generation (SFG) in another MgO:PPLN. The performance, including the quality-factor (Q-factor) and extinction ratio (ER), of the proposed multifunctional logic device is also simulated.

OCIS codes: 190.0190, 200.3760, 130.3730.
doi: 10.3788/COL201311.061901.

All-optical signal processing techniques are extremely important in advance optical networks because they can deal with the ultrahigh speed optical signals, contrary to currently used electronic devices with limited speed of signal processing[1]. Logic gates play an important role in all-optical signal processing, such as various logical function operations, signal regeneration, pattern recognition addressing, header recognition, data encoding, and encryption[2,3]. Consequently, all-optical logic gates have become in-demand in scientific research. Several basic logic gates, such as AND[4,5], OR[6], NOT[7], NAND[7,8], and XOR[9−11] gates, have been proposed and experimentally demonstrated in various devices, including semiconductor optical amplifiers[6,12,13], semiconductor micro-resonator[14], fiber nonlinearity, and periodically poled lithium niobate (PPLN)[4,7,11].

Recently, PPLN has become one of the foci of various scientific research groups because of its complete transparency, absence of excess noise, ultra-fast response, and other attractive properties[4]. Several mutations of PPLN, such as pure PPLN, PPLN diffused by Ti[7], and MgO-doped PPLN[15], exhibit diverse desirable properties. With all these properties, various second-order nonlinearities and their cascading nonlinear processes can be potentially applied to high-speed all-optical signal processing, such as all-optical wavelength conversion, optically gated switching, and logic gate.

We propose simultaneous AND, NOR, and XNOR logic gates with pulse signals of τ_0=3.73 ps at 40 Gb/s in this letter by employing two MgO:PPLNs. In our proposal, cascaded second harmonic and difference-frequency generation (cSHG/DFG), cascading sum-frequency and difference-frequency generation (cSFG/DFG), and single sum-frequency generation (SFG) in PPLNs are exploited. The performance of the logic gates, including their quality-factors (Q-factors) and extinction ratios (ERs), is also analyzed through numerical simulation.

Table 1 shows the truth table for the AND, NOR, and XNOR logic gates.

The proposed logic device is based on two MgO:PPLNs, in which one uses the cSHG/DFG and cSFG/DFG processes, simultaneously occurring at the same MgO:PPLN for broadband quasi-phase matching (QPM) employment[16−18], and the other uses the SFG process with narrow band QPM[19]. The schematic diagram for the logic gate device is illustrated in Fig. 1. Two input pulse signals, S1 and S2, at 40 Gb/s, and a continuous wave (CW) for control light are injected into the 1st MgO:PPLN waveguide. For the 2nd MgO:PPLN, the filtered control light from the 1st MgO:PPLN, together with a CW pump light, is launched.

In the 1st MgO:PPLN, if signals S1 and S2 are located within the proper wide bandwidth of type I QPM second harmonic generation (SHG)[15−17], the second harmonic waves 1 (SH1) and 2 (SH2) will be generated, respectively. In addition, if S1 and S2 appear in the SFG bandwidth, they will participate in the SFG process, generating a one sum-frequency (SF) photon by simultaneously annihilating one S1 photon and one S2 photon. The control light is a CW and it will interact with SH1, SH2, and SF through the DFG processes as long as they are in existence. As a result, three DFG processes will by annihilating one SH1/SH2/SF photon to create one control photon and one idler1/idler2/idler3 photon. To

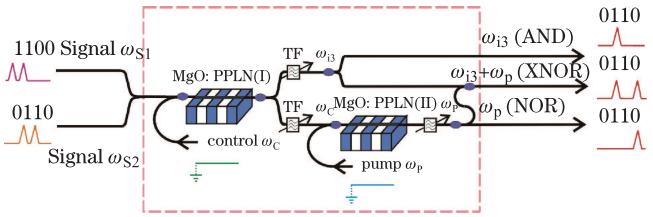

Fig. 1. Schematic diagram of simultaneous AND, NOR, and XNOR logic gates. TF: tunable filter.

Table 1. Truth Table of Logic Gates

Input		Logic Gates		
S1	S2	AND	NOR	XNOR
0	0	0	1	1
0	1	0	0	0
1	0	0	0	0
1	1	1	0	1

Table 2. Parameters of These Two MgO: PPLNs

Symbol	Description	Value
Λ_1 (μm)	Poling Period of the 1st MgO:PPLN	20.07
L_1 (cm)	Length of the 1st MgO:PPLN	5
$d_{1,\mathrm{eff}}$ (pm/V)	Effective Coefficient of the 1st MgO:PPLN	2.99
$A_{1,\mathrm{eff}}$ (μm^2)	Effective Interaction Area of the 1st MgO:PPLN	30
Λ_2 (μm)	Poling Period of the 2nd MgO:PPLN	20.07
L_2 (cm)	Length of the 2nd MgO:PPLN	4.5
$d_{2,\mathrm{eff}}$ (pm/V)	Effective Coefficient of the 2nd MgO:PPLN	16.5
$A_{2,\mathrm{eff}}$ (μm^2)	Effective Interaction Area of the 2nd MgO:PPLN	30

achieve a high DFG conversion efficiency, the control light should experience neither SHG nor SFG with S1 or S2.

When both S1 and S2 are "1", light SH1, SH2, and SF will be created, thus triggering the following three DFG processes, yielding control photons as well as idler1, idler2, and idler3 photons. However, only light SH1 or SH2 exists when S1 or S2 exists without each other. In this sense, only the control and idler1 photons, or control and idler2 photons will be created, indicating that no idler3 photons are found but control photons. If both S1 and S2 are "0", no SHG, SFG, and DFG processes will occur, which results in the absence of created control, idler1, idler2, and idler3 photons. Considering the above processes, which imply that idler3 exists only when S1 and S2 are "1" simultaneously, along with the information presented in Table 1, idler3 is hence suitable for the output of the AND gate. Moreover, as long as S1 and S2 are not "0" simultaneously, cont-rol photons will be created, giving overshoots to the CW control light, which indicates that information relating to OR operation is transferred to the control light.

For the 2nd MgO:PPLN, a new CW light pump was launched in together with the control signal. The wavelengths of these two lights meet the SFG QPM condition through type 0 narrow band QPM interaction. With the control light carrying the OR gate information, the SFG process, which acts as the NOT operation, will create notches on the CW pump light where the control light has overshoots. If a suitable length of the 2nd MgO: PPLN waveguide is selected, the SFG process can deplete pump light completely at those points where the control light has overshoots. Acting as the NOT operation on control light, the 2nd MgO:PPLN makes the output pump light non-zero only when both S1 and S2 are "0". As indicated in Table 1, the output pump light acts just as the output of the NOR gate. Moreover, by combining the output lights of the AND and NOR gates, we naturally obtained the XNOR gate, as shown in Table 1.

To realize all these gates, optimum parameters such as λ_{S1}, λ_{S2}, λ_C, and λ_P should be chosen in our proposal. The coupled-mode equations[20] describing the SHG, SFG, and DFG processes in the 1st MgO:PPLN and the SFG process in the 2nd MgO:PPLN can be numerically solved using the finite difference beam propagation method (FD–BPM)[21]. Proper operating parameters of these two MgO:PPLNs are chosen for our simulation, some of which are shown in Table 2.

The blue line in Fig. 2 plots the SHG conversion efficiency versus the input signal wavelength in the 1st MgO:PPLN. The bandwidth (full-width at half-maximum (FWHM)) for the high SHG conversion efficiency is approximately 15 nm centered at 1.561 μm. Considering the requirement for wavelength of input signals S1 and S2, which indicate that both signals S1 and S2 should have high SHG conversion efficiencies, we selected $\lambda_{S1} = 1.557$ μm and $\lambda_{S2} = 1.565$ μm. After λ_{S1} and λ_{S2} have been fixed, we also plot two SFG conversion efficiency curves, i.e., with $\lambda_{S1} = 1.557$ μm and $\lambda_{S2} = 1.565$ μm. These two SFG curves confine a wavelength region, in which the corresponding input signal should be chosen to achieve high SFG conversion efficiency. Moreover, the SHG and the SFG curves limit the control light, the wavelength of which should be chosen at regions where neither the SHG nor the SFG process could occur if interacting with any of the two input signals S1 and S2. In this sense, λ_C was set at 1.585 μm.

After the wavelength of the input control light was fixed, we selected the proper wavelength of the pump light launched in the 2nd MgO:PPLN. The SHG and the SFG conversion efficiencies with $\lambda_C = 1.585$ μm are demonstrated in Fig. 3. The blue curve (SHG) indicates that $\lambda = 1.568$ μm meets the SHG conversion efficiency condition best, which also indicates that both the input control signal and the pump signal should avoid the tiny wavelength region around $\lambda = 1.568$ μm. The green curve in Fig. 3 indicates that $\lambda = 1.552$ μm meets the

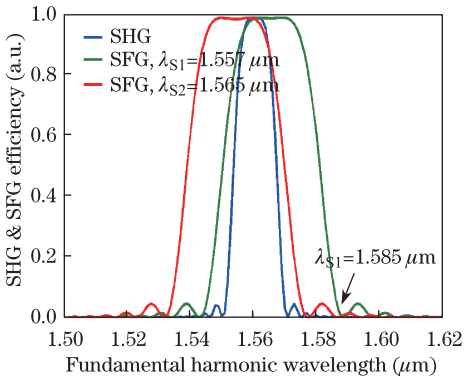

Fig. 2. (Color online) SHG and SFG conversion efficiencies in the 2nd MgO:PPLN.

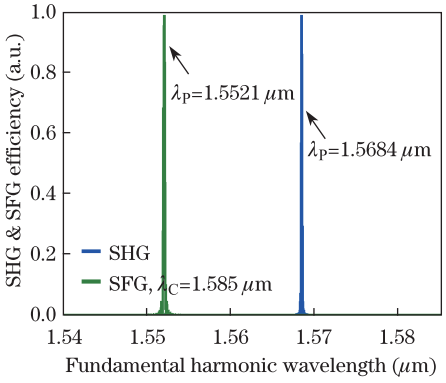

Fig. 3. (Color online) SHG and SFG conversion efficiencies for the 1st MgO:PPLN.

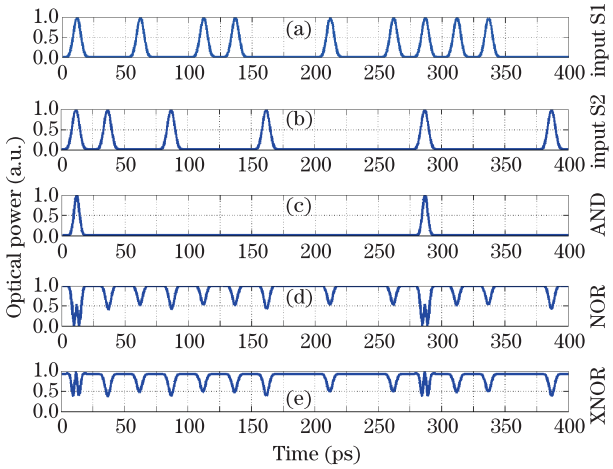

Fig. 4. Temporal waveforms of AND, NOR, and XNOR gates at 40 Gb/s. (a) Signal S1 and (b) signal S2; outputs of the (c) AND, (d) NOR, and (e) XNOR gates.

highest SFG conversion efficiency with $\lambda_C = 1.585$ μm. In this sense, λ_P was set at 1.552 μm.

The input signals S1 and S2 were assumed to be Gaussian-shaped with amplitudes $A(0,t)$ used in our simulation expressed as

$$A(0,t) = \sqrt{P_0}\exp\left(-2\ln 2\frac{t^2}{\tau_0^2}\right),$$

where τ_0=3.73 ps is the FWHM of the signal pulse, and P_0=200 mW is the peak power of the pulse signal. Additionally, input signals S1 and S2 were considered as synchronized independent 2^7–1 pseudo-random binary sequence return-to-zero (RZ) data streams, with 30-dB ER and 40-dB signal-to-noise ratio (SNR). Both the control light in the 1st MgO:PPLN and the pump light in the 2nd MgO:PPLN are CWs with powers of P_C=60 mW and P_P= 50 mW, respectively.

The propagation and conversion characteristics of all involved waves were simulated based on the above model and parameters. In the following simulation results, some typical temporal characteristics of designed logic gates are shown. The waveforms of input signals S1 and S2 and the outputs of AND, NOR, and XNOR gates are plotted in Fig. 4. The input sequence of signal S1 is "1010, 1100, 1011, 1100", and that of signal S2 is "1101, 0010, 0001, 0001". Similar to the truth value principle shown in Table 1, the corresponding output sequences of the AND, NOR, and XNOR gates are "1000, 0000, 0001, 0000", "0000, 0001, 0100, 0010", and "1000, 0001, 0101, 0010", respectively.

The eye diagrams for signal S1, AND, NOR, and XNOR logic gates are illustrated in Fig. 5. The Q-factor and ER, which are defined as $Q = 20\lg[(\mu_1 - \mu_0)/(\sigma_1 + \sigma_0)]$ and ER=$10\lg(\mu_1/\mu_0)$, respectively, are used to evaluate the operation performance. μ_1 and μ_0 are the average powers of logical "1" and "0" of the eye diagrams at the best sampling time, and σ_1 and σ_0 are the corresponding standard deviations.

Table 3 shows the corresponding Q-factor and ER of the AND, NOR, and XNOR gates.

Both Fig. 5 and Table 3 show that the AND gate has nice eye opening and high Q-factor and ER. By contrast, the eye opening, Q-factor, and ER of the NOR gate are not as large as those of the AND gate's, which is mainly caused by the two cascaded effects in these two MgO:PPLNs and non-equivalent coupled coefficients between the SHG processes and the SFG process in the 1st MgO:PPLN. The non-equivalent coupled coefficients of the SHG and SFG processes render different amounts of created control photons, then the height of the overshoots to the CW control light are not the same for the SHG and SFG processes. When those overshoots propagate in the 2nd MgO:PPLN, they consume different amounts of CW pump light because of their different powers. Thus, the SFG process reaches the turning point as the length of propagation gets longer. This condition indicates that the SFG process will turn into a DFG process, providing extra photons to the control lights generated through SFG in the 1st MgO:PPLN. However, these control lights generated through SHG in the 1st MgO:PPLN, which are smaller in power than those generated by the SFG process, have not arrived at the turning point. Hence, the waveforms of NOR are created (Fig. 4). The Q-factor of the NOR gate is thus not good enough. Moreover, the performance of the XNOR gate is not so good, that is, it has small eye opening and low values for the Q-factor and ER, which are basically caused by two aspects. Firstly, the performance of the NOR gate is not desirable because of the non-zero power corresponding to the "0"

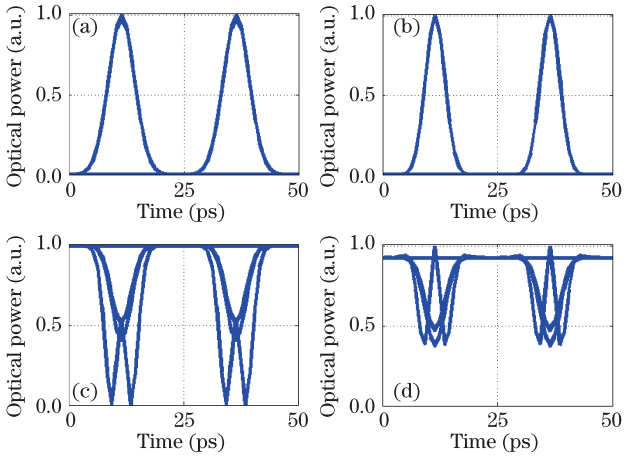

Fig. 5. Eye diagrams of the AND, NOR, and XNOR gates at 40 Gb/s. (a) Signal S1 or S2, outputs of the(b)AND, (c) NOR gate, and (d) XNOR gates.

Table 3. *Q*-factor and ER of Logic Gates

	AND	NOR	XNOR
Q-factor	38.079 dB	19.483 dB	14.976 dB
ER	49.825 dB	3.098 dB	3.322 dB

data, which largely influences the performance. Secondly, the waveforms of the AND and NOR gates are not of the same form after propagation in MgO: PPLN. Different shapes with different pulse widths cause these two waveforms to become narrow in the central area. Hence, the distortion of optical pulse is not as severe as in the narrow band PPLN[22] because the wide band preserves most parts of the optical pulse spectra. In our calculation, the difference of the total energy propagating along the PPLN waveguide is small and does not exceed 0.9%. This result verifies that the accuracy of the simulations is acceptable, and the law of energy conservation is also satisfied.

In conclusion, a multi-functional logic device that can realize AND, NOR, and XNOR logic gates simultaneously is simulated numerically. The influence of input signal power and input signal wavelength on the performance, that is, *Q*-factor and ER of the logic gates, is theoretically analyzed. Simulation results show that with RZ input signal of τ_0=3.73 ps at 40 Gb/s, the performance of the AND gate is very good, in contrast to the ordinary performances of the NOR and XNOR gates. Combined with other devices based on PPLN with applications in all-optical wavelength conversion[16,17], optical delay[23], and so on, a multi-functional logic gate device based on PPLNs in our proposal may be potentially useful for constructing on-chip all-optical high-speed integrated devices in advance high-speed all-optical signal processing, optical interconnects, and computing[24].

This work was supported by the National Natural Science Foundation of China (No. 11174204) and the Shanghai Jiaotong University Innovative Practical Program.

References

1. D. Cotter, R. J. Manning, K. J. Blow, A. D. Ellis, A. E. Kelly, D. Nesset, I. D. Phillips, A. J. Poustie, and D. C. Rogers, Science **286,** 1523 (1999).
2. R. P. Webb, X. Yang, R. J. Manning, G. D. Maxwell, A. Poustie, S .Lardenois, and D. Cotter, J. Lightwave Technol. **27,** 2240 (2009).
3. G. P. Agrawal, *Fiber-Optic Communication Systems* (Wiley, New York, 2002).
4. J. Wang, J. Sun, Q. Sun, D. Wang, X. Zhang, D. Huang, and M. M. Fejer, IEEE Photon. Technol. Lett. **20,** 211 (2008).
5. P. Andalib and N. Granpayeh, J. Opt. Soc. Am. B **26,** 10 (2009).
6. H. Dong, Q. Wang, G. Zhu, J. Jaques, A. Piccirilli, and N. Dutta, Opt. Commun. **242,** 479 (2004).
7. Y. L. Lee, B.-A. Yu, T. J. Eom, W. Shin, C. Jung, Y.-C. Noh, J. Lee, D.-K. Ko, and K. Oh, Opt. Express **14,** 2776 (2006).
8. B. Nakarmi, M. Rakib-Uddin, T. Q. Hoai, and Y. H. Won, IEEE Photon. Technol. Lett. **23,** 236 (2011).
9. J. Xu, X. L. Zhang, Y. Zhang, J. J. Dong, D. M. Liu, and D. X. Huang , J. Lightwave Technol. **27,** 5268 (2009).
10. J. Wang, Q. Z. Sun, and J. Q. Sun, Opt. Express **17,** 12555 (2009).
11. Y. X. Zhang, Y. P. Chen, and X. F. Chen, Appl. Phys. Lett. **99,** 161117 (2011).
12. T. A. Ibrahim, R. Grover, L.-C. Kuo, S. Kanakaraju, L. C. Calhoun, and P.-T. Ho, IEEE Photon. Technol. Lett. **15,** 1422 (2003).
13. L. Yi, W. Hu, H. He, Y. Dong, Y. Jin, and W. Sun, Chin. Opt. Lett. **9,** 030603 (2011).
14. J. H. Kim, Y. T. Byun, Y. M. Jhon, S. Lee, D. H. Woo, and S. H. Kim, Opt. Commun. **218,** 345 (2003).
15. J. Zhang, Y. Chen, F. Lu, W. Lu, W. Dang, X. Chen, and Y. Xia, Appl. Opt. **46,** 7792 (2007).
16. J. F. Zhang, Y. P. Chen, F. Lu, and X. F. Chen, Opt. Express **16,** 6957 (2008).
17. M. J. Gong, Y. P. Chen, F. Lu, and X. F. Chen, Opt. Lett. **35,** 2672 (2010).
18. J. Xie, Y. Chen, W. Lu, and X. Chen, Chin. Opt. Lett. **9,** 041902 (2011).
19. X. L. Zeng, X. F. Chen, Y. P. Chen, Y. X. Xia, and Y. L. Chen, Opt. Laser Technol. **35,** 187 (2003).
20. T. Suhara and M. Fujimura, *Waveguide Nonlinear-Optic Devices* (Springer-Verlag, Berlin, 2003).
21. K. Okamoto, *Fundamentals of Optical Waveguides* (Academic Press, Waltham, 2006) chap. 7.
22. Y. Wang, J. Fonseca-Campos, C. Q. Xu, S. Q. Yang, E. A. Ponomarev, and X. Y. Bao, Appl. Opt. **45,** 5391 (2006).
23. W. J. Lu, Y. P. Chen, L. H. Miu, X. F. Chen, Y. X. Xia, and X. L. Zeng , Opt. Express **16,** 355 (2008).
24. H. J. Caulfield and S. Dolev, Nat. Photon. **4,** 261 (2012).